Interaction of the $6p^2\ ^1S_0$ broad resonance with $5dnd\ J=0$ autoionizing resonances in barium

M. A. Kalyar,* M. Rafiq, and M. A. Baig†
Atomic and Molecular Physics Laboratory, Department of Physics, Quaid-i-Azam University, 45320 Islamabad, Pakistan
(Received 24 August 2009; published 12 November 2009)

We present even-parity autoionizing resonances in barium using two-step laser excitation via $5d6p\ ^1P_1$ intermediate level covering the energy region from the first ionization threshold to the $5d\ ^2D_{5/2}$ limit. The data are achieved using an atomic beam apparatus in conjunction with a time-of-flight mass spectrometer and a Nd:YAG pumped dye laser system. True line shape of the $6p^2\ ^1S_0$ autoionizing resonance at $44\ 850 \pm 50\ \mathrm{cm}^{-1}$, its width ($980 \pm 50\ \mathrm{cm}^{-1}$), and the absolute value of photoionization cross section (185 ± 35 Mb) are reported. A combination of parallel and perpendicular polarization vectors of the exciting and the ionizing dye lasers reveals unambiguous J-value assignments of the excited states. The interactions between the $6p^2\ ^1S_0$ broad feature with the $5d_{5/2}nd\ J=0$ Rydberg series have been simulated using the phase-shifted multichannel quantum defect theory.

DOI: 10.1103/PhysRevA.80.052505 PACS number(s): 32.30.Jc, 32.80.Ee, 32.80.Zb

I. INTRODUCTION

The level structure based on the $6p^2$ configuration in barium yields $^3P_{0,1,2}$, $^1D_2$, and $^1S_0$ levels. Their energies and assignments are well established except the $6p^2\ ^1S_0$ level that remained controversial and has therefore attracted considerable attention during the last couple of decades. Initially, Moore [1] designated the level at $38\ 663\ \mathrm{cm}^{-1}$ as $6p^2\ ^1S_0$ and later the level at $34\ 370.78\ \mathrm{cm}^{-1}$ was given this assignment by Moore [2]. Subsequently, Rubbmark *et al.* [3] studied the $6sns\ ^1S_0$ Rydberg series and identified a perturbing level at $38\ 663.75\ \mathrm{cm}^{-1}$ as $6p^2\ ^1S_0$. Aymar *et al.* [4] reinvestigated the even-parity $J=0$ levels and assigned the above-mentioned level as $6s10s\ ^1S_0$ and predicted that the $6p^2\ ^1S_0$ seems to lie at $45\ 320\ \mathrm{cm}^{-1}$, above the $6s$ ionization threshold. Wynne and Armstrong [5] studied the systematic trends in alkaline-earth metal atoms using Multichannel Quantum Defect Theory (MQDT) and assigned the $6p^2\ ^1S_0$ level at $38\ 924\ \mathrm{cm}^{-1}$. Based on the semiempirical calculations, Camus *et al.* [6] removed this ambiguity by assigning the level at $38\ 924\ \mathrm{cm}^{-1}$ as $5d6d\ ^1S_0$, which was earlier assigned as $6s10s\ ^1S_0$ by Rubbmark *et al.* [3] and $6p^2\ ^1S_0$ by Armstrong *et al.* [7]. Moreover, they concluded that the $6p^2\ ^1S_0$ level is still unknown and should be searched elsewhere.

The first experimental evidence of the $6p^2\ ^1S_0$ level was provided by Aymar *et al.* [8] who observed a broad feature above the first ionization threshold centered around $44\ 800\ \mathrm{cm}^{-1}$ and $\approx 300\ \mathrm{cm}^{-1}$ broad. This identification was based on the MQDT analysis of the interaction among the $6pnp\ ^1S_0$ series and the $6s\varepsilon s\ ^1S_0$ continuum. Bartschat *et al.* [9] reported the photoionization from the $6s6p\ ^1P_1$ excited state using R-matrix calculations and surprisingly the $6p^2\ ^1S_0$ broad resonance was missing; their calculations predicted a broad resonance above the $5d_{5/2}$ threshold. This again put a question mark on the location of the $6p^2\ ^1S_0$ resonance. Subsequently, Bartschat and Greene [10] improved their R-matrix calculations by considering the short-range correlation and relaxation effects of the $6p$ orbital including continuum-continuum configurations and predicted the position of the $6p^2\ ^1S_0$ resonance at about 374 nm (photon wavelength relative to the $6s6p\ ^1P_1$ excited state). Greene and Aymar [11] calculated the partial photoionization cross section for the $5d6p\ ^1P_1\ J=0$ of barium in the energy range $42\ 000$–$47\ 000\ \mathrm{cm}^{-1}$ using multichannel quantum defect theory and eigenchannel R-matrix calculations. Recently, the polarization-dependent photoionization cross sections of two even-parity excited states $5d6d\ ^3D_1$ and $6s7d\ ^3D_2$ of barium are reported by Li and Budker [12].

The objectives of this present study are to obtain the line profile of the $6p^2\ ^1S_0$ autoionizing resonance and to unfold the interaction of this broad feature with the neighboring $5dnd\ J=0$ autoionizing resonances. Exploiting the two-step excitation-ionization technique via the $5d6p\ ^1P_1$ intermediate level we report the photoionization spectra from the $6s$ ionization threshold to the $5d_{5/2}$ threshold using the polarization vectors of the exciting and the ionizing dye lasers either parallel or perpendicular to each other, in two different sets of measurements, to achieve unambiguous level assignments. We have also performed four-channel quantum defect theory calculations to simulate the interaction between the $6p^2\ ^1S_0$ broad resonance with the $5d_{3/2,5/2}$ Rydberg states of the same J values. The phenomena of q reversal in the Rydberg transitions in the vicinity of the perturbing broad feature are experimentally demonstrated.

II. EXPERIMENTAL DETAILS

The experimental setup, shown in Fig. 1, is the same as described in our earlier papers [13–15]. A well-collimated atomic beam of barium was produced at a constant temperature (≈ 900 K) that travels from the lower to the upper part in the vacuum chamber and passes through the center of the ionization and extraction region of an in-house built time-of-flight (TOF) mass spectrometer. The barium atomic beam was irradiated with the exciter laser to populate the $5d6p\ ^1P_1$ excited state, followed by an ionizer laser with a delay of

*Present address: Department of Physics, GC University Faisalabad, Pakistan.
†Corresponding author. FAX: +92 51 9210256; baig@qau.edu.pk; baig77@gmail.com

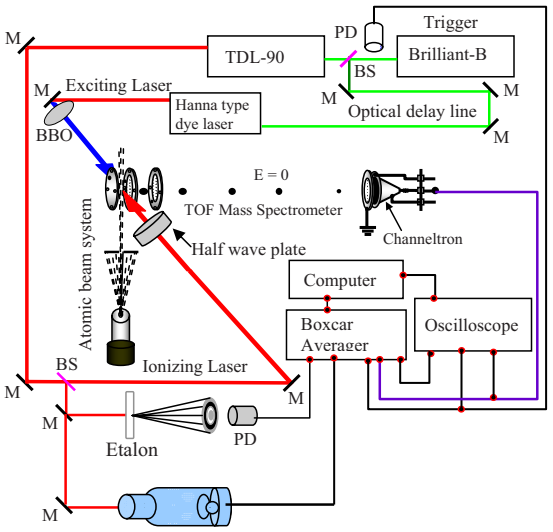

FIG. 1. (Color online) Schematic of the experimental setup.

about 6 ns to separate the excitation and ionization processes. Both the dye lasers were pumped by a common Nd:YAG laser (Brilliant B, Quantel). In the first step the atoms were resonantly excited to the doubly excited $5d6p\ ^1P_1$ state using an open cavity Hanna-type [16] dye laser (pulse length 5 ns; bandwidth $\approx 0.3\ \mathrm{cm}^{-1}$) charged with LDS-698 and the uv photons at 350.2 nm (bandwidth $\approx 0.6\ \mathrm{cm}^{-1}$) were produced by frequency doubling the 700.4 nm wavelength by a beta barium borate crystal. In the second step, these excited atoms were ionized with the probe dye laser (TDL-90, Quantel) (bandwidth $\approx 0.1\ \mathrm{cm}^{-1}$) covering the energy region from 42 035 to 47 720 cm^{-1}. Different dyes such as LDS-698, DCM, Rhodamin 640, Rhodamin 610, Rhodamin 590, Flourescen 548, and Coumarine 500 were used to cover the entire region of interest. Some mixtures of different dyes were also used to overlap the scanning region and to maintain a constant intensity of the ionizing laser. The wavelength region is scanned when both the exciting and the ionizing lasers were linearly polarized. By inserting a half wave plate in the path of the ionizing laser its polarization vector was adjusted either parallel or perpendicular to that of the first dye laser revealing autoionizing states of different total angular momentum quantum numbers.

III. RESULTS AND DISCUSSION

The photoionization spectra of barium have been recorded via the $5d6p\ ^1P_1$ intermediate level by scanning the probe laser from the $6s$ threshold to the $5d\ ^2D_{3/2}$ ionization threshold. The spectra are recorded by adjusting the polarization vectors of the pump and the probe dye lasers either parallel or perpendicular to each other. The selection of combinations of polarization vectors of the two laser beams permits to access the final states with different total angular momentum. The probability of absorption of a photon is proportional to the square of the modulus of the dipole matrix element [17,18]:

$$W_{n_0 l_0 J_0 m_0 \to n_1 l_1 J_1 m_1} \propto |\langle n_1 l_1 J_1 M_1 | D_q | n_0 l_0 J_0 M_0 \rangle|^2.$$

Here J and M are the total angular momentum and its projection, respectively, and D_q are the spherical components; $q=0$ applies to linearly polarized light and ± 1 to circularly polarized light. The Wigner-Eckart theorem leads to the separation of the matrix element into a geometrical and physical part; the angles are incorporated in the coefficients and the physical part is expressed in terms of a reduced matrix element:

$$\langle n_1 l_1 J_1 M_1 | D_q | n_0 l_0 J_0 M_0 \rangle = (-1)^{J_1 - M_1} \begin{pmatrix} J_1 & 1 & J_0 \\ -M_1 & q & M_0 \end{pmatrix} \times \langle n_1 l_1 J_1 || D || n_0 l_0 J_0 \rangle.$$

The dipole matrix element describing the absorption of a second photon in the second step can be described as

$$\langle n_2 l_2 J_2 M_2 | D_q | n_1 l_1 J_1 M_1 \rangle = (-1)^{J_2 - M_2} \begin{pmatrix} J_2 & 1 & J_1 \\ -M_2 & q & M_1 \end{pmatrix} \times \langle n_2 l_2 J_2 || D || n_1 l_1 J_1 \rangle.$$

Only those values of the total angular momentum via single photon absorption are allowed for which the two $3j$ symbols in the above two equations are nonvanishing. In the first-step excitation from the ground state $6s^2\ ^1S_0$ ($J=0$ and $M_j=0$) with the linearly polarized light, the $5d6p\ ^1P_1$ ($J=1$ and $M_j=0$) is populated. When the polarization vector of the second-step laser beam is adjusted parallel to that of the first-step laser, the final states of $M_j=0$, $J=0$ and 2 are allowed while $J=1$ is forbidden. In the case of perpendicular polarization vectors, the excited states with $M_j=\pm 1$, $J=1$ and 2 are allowed but $J=0$ is forbidden. Thus, the $6p^2\ ^1S_0$ excited state is only accessible from the $5d6p\ ^1P_1$ intermediate state when the polarization vectors of both the dye lasers are parallel to each other and it will be forbidden in the case of perpendicular polarization arrangement.

The lifetime of the $5d6p\ ^1P_1$ level is 12.17 ns [19]; the scanning laser pulse is therefore delayed by ≈ 6 ns with respect to the exciting laser to ensure a pure two-step ionization and to avoid any ionization caused by the first laser of any state populated by the scanning laser. The pulse energy of the exciting laser was kept $\approx 5\ \mu$J to obstruct the two-photon ionization hitherto provided sufficient population of the excited state. The energy of the ionizing laser at 737 nm wavelength was $\approx 300\ \mu$J and it is divided into three parts to record the optogalvanic spectra from a hollow cathode lamp (wavelength standards), fringes from a Fabry-Perot etalon (relative energy markers), and photoion signal from a channeltron. The intensity of the scanning laser was monitored through a fast photodiode which had a linear response for the laser intensities. It was ensured that the intensity of the scanning laser remained nearly constant and no ion signal got saturated throughout the scanning region.

In Fig. 2 we show the photoionization spectra of barium excited from the $5d6p\ ^1P_1$ intermediate level covering the energy region 42 000–46 000 cm^{-1}. Each and every observed line in this region is identified with the help of the laser polarization selection rules. The lines that are present in

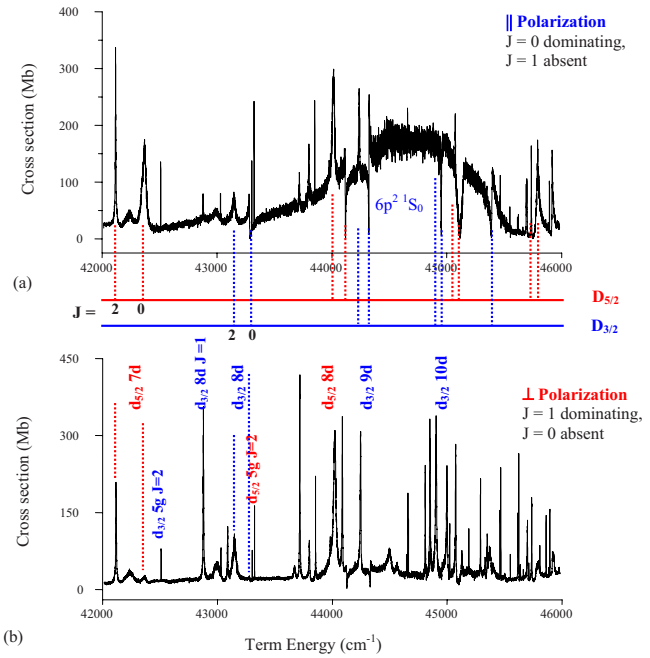

FIG. 2. (Color online) The photoionization spectra recorded from the $5d6p\ ^1P_1$ intermediate level in the region 42 000–46 000 cm^{-1} (a) with parallel polarization vectors of the exciting and the ionizing lasers. (b) When the polarization vector of the ionizing beam is made perpendicular to that of the exciting laser, the $J=0$ broad feature is absent in this case. The $J=2$ resonances are present in both the spectra that enabled us to assign the J values of the resonances.

the case of parallel as well as in the case of perpendicular polarization vectors of the dye lasers are recognized as $J=2$. The lines that are present only for the perpendicular polarizations of the two lasers are labeled with $J=1$. However, the lines that appear only when the polarization vectors of both the laser beams are parallel are assigned $J=0$. The term energies of the autoionizing resonances have been determined by adding the energy 28 554.26 cm^{-1} of the $5d6p\ ^1P_1$, intermediate state to the excitation energy of the scanning laser. The dye laser was scanned with a motor step of 0.02 cm^{-1} and the term energies are measured with an accuracy of 0.2 cm^{-1}. The term energies of theses resonances are in good agreement with that of Camus *et al.* [20]. If we subtract these resonances from the spectrum recorded with the parallel combination of the two lasers, we retrieve the true line shape of the $6p^2\ ^1S_0$ autoionizing resonance. The presence of the $6p^2\ ^1S_0$ resonance can also be seen in the spectra for the parallel polarizations of the two lasers in the work of Lange *et al.* [21] and Wood *et al.* [22] for the photoionization from the $6s6p\ ^1P_1$ excited state.

The observed spectra are arranged into Rydberg series attached to the $5d_{3/2,5/2}$ ionic levels of barium [23,24]. The upper spectrum was recorded by adjusting the polarization vectors of the exciting as well as the ionizing lasers parallel where the levels predominantly are $J=0$ and 2 but $J=1$ are very weak. The lower spectrum was recorded by adjusting the polarization vector of the ionizing laser beam perpendicular to that of the exciting laser. In this case the $J=0$ levels are very weak whereas the dominating levels possess

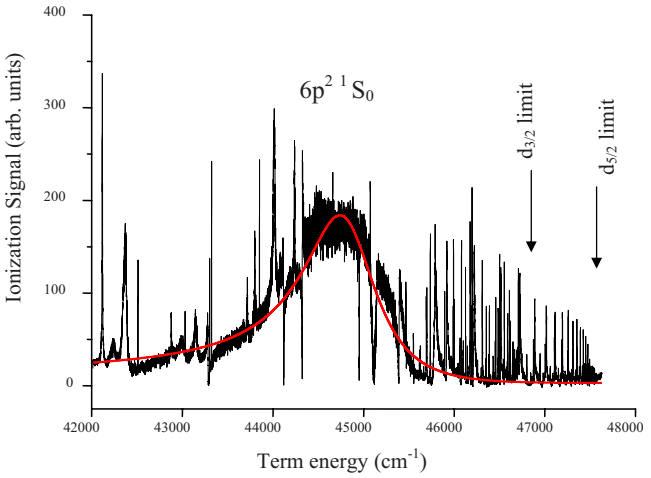

FIG. 3. (Color online) The photoionization spectrum of barium along with the least-squared fit of Fano's relation [25] to the broad feature ascribed as $6p^2\ ^1S_0$ autoionizing resonance.

$J=2$ and 1. Interestingly, the forbidden $J=0$ or 1 resonances are present in the perpendicular or parallel polarizations spectrum, respectively, but their intensities are much lower as compared to the allowed transitions for that combination of polarizations. These forbidden lines are caused either by the admixture of the elliptically polarized light as the light is not hundred percent linearly polarized or due to hyperfine depolarization as reported by Wood *et al.* [22]. The $J=2$ lines are present in both the spectra that enabled us to assign the J values of the resonances unambiguously. As in the upper trace the dominating lines possess $J=0$; therefore, the superimposed broad feature is identified as the $6p^2\ ^1S_0$ autoionizing resonance which completely disappears in the lower trace. In addition, a very sharp line, $5d_{5/2}5g\ J=2$, appears in both the spectra with varying intensity. The $d_{3/2}8d\ J=1$ line is prominent in the lower spectrum but very weak in the upper trace. There are a few other weak lines in this region that are identified as members of the $d_{3/2,5/3}ns$ series.

Figure 3 shows the experimentally recorded spectrum along with a solid line which is the least-squares fit of the relation to describe the cross section of an isolated autoionizing resonance [25]:

$$\sigma(\varepsilon) = \sigma_a \frac{(q+\varepsilon)^2}{1+\varepsilon^2} + \sigma_b, \quad \varepsilon = \frac{(E-E_r)}{\Gamma/2}. \tag{1}$$

Here $\sigma(\varepsilon)$ represents the absorption cross section; σ_a and σ_b are the portions of the cross section of the continuum which interacts and does not interact with the discrete level, respectively; q is the line profile index parameter; ε measures the departure of the incident photon energy E from the resonance energy E_r; and Γ reflects the width of the autoionizing resonance. The resonance energy, width, and the line profile index parameter of the $6p^2\ ^1S_0$ resonance and the other $J=0$ resonances in the vicinity of this resonance have been extracted by the least-squares fitting of this relation. The best fit yields the energy position=44 850 ± 50 cm^{-1}, width=980 ± 50 cm^{-1}, and $q=-5.4\pm2$ for the $6p^2\ ^1S_0$ resonance. This energy position is in good agreement with the

value 44 800 cm^{-1} reported by Aymar *et al.* [8] while the width is nearly three times larger than their reported value. This difference is attributed to the fact that Aymar *et al.* [8] considered this resonance localized in a very small energy span contrary to its actual spread. The resonance energy position is also in good agreement with the calculated value by Greene and Aymar [11]; however, the experimental width is much too large.

We have observed an excellent example of q reversals [26–28] as the sharp $5d_{3/2}nd$ $J=0$ $(8 \leq n \leq 10)$ autoionizing resonances sweep across the broad $6p^2\ ^1S_0$ resonance. In Figs. 4(a)–4(c) we show the line profiles of the $5d_{3/2}8d$ and $5d_{3/2}9d$ and $5d_{3/2}10d$ resonances along with the least-squares-fitted curves. Interestingly, the $5d_{3/2}nd$ $J=0$ lines in the vicinity of the $6p^2\ ^1S_0$ resonance exhibit reversals in the profile symmetry; the sign of the q parameter changes from $n=8$ to $n=11$. The $5d_{3/2}8d$ $J=0$ and $5d_{3/2}9d$ $J=0$ resonances lying on the lower energy side of the $6p^2\ ^1S_0$ resonance possess $q=-1.1$ and $+1.0$, respectively, while the next member of this series lying close to the peak energy position of $6p^2\ ^1S_0$ looks like a window resonance having $q \approx 0$. The best fit to the $5d_{3/2}10d$ resonance yields $q=0.05$. The $5d_{3/2}11d$ resonance, lying above $6p^2\ ^1S_0$, appears with a positive q value and then the next members of the series that lie away from the $6p^2\ ^1S_0$ resonance regain the regular Fano-type resonance behavior. An identical situation persists for the $d_{5/2}nd$ $J=0$ autoionizing resonances (see Fig. 2). Keller *et al.* [29] recorded the photoionization spectra of barium over a limited region from the $5d6p\ ^1P_1$ and $6s6p\ ^1P_1$ excited states and extracted the profile parameters by fitting the Fano relation to these resonances. A comparison of our results with that of Keller *et al.* [29] is presented in Table I. The width and q value of the $5d_{3/2}9d$ $J=0$ resonance are in excellent agreement whereas the width and q value of the $5d_{5/2}8d$ $J=0$ resonance are smaller than that of Keller *et al.* [29].

In Table II we enlist the lines attached to the $5d7d$ and $5d8d$ configurations. Three lines are assigned to the level structure based on the $5d7d$ configuration including the well studied perturber $5d7d\ ^1D_2$ assigned in the jj coupling as $(5/2,3/2)_2$; the other lines lie well below the ionization threshold. Nine lines are identified attached to the $5d8d$ configuration. Here, a completely resolved structure for the $5d8d$ configuration has been reported with unambiguous level assignments using the polarization spectroscopy. The other lines in this spectrum shown in Fig. 2 belong to the $5dns$, nd, and ng configurations. The level assignments have been made using the jj coupling as it is a more appropriate coupling scheme to designate the levels built on the $5d$-ionic level of barium due to its larger spin-orbit interaction contribution.

It is worth to mention that we have acquired the data using a time-of-flight mass spectrometer and as a result we manage to see the zero in the cross section very clearly. We have also determined the absolute value of the photoionization cross section at the peak of the strong resonance using the saturation technique.

A. Photoionization cross-section measurements

In order to put the observed spectra on an absolute scale, we have measured the absolute value of the photoionization cross section of the $5d6p\ ^1P_1$ level at the peak of the $5d7d$ $(5/2,5/2)_2$ resonance for the parallel and the perpendicular polarization vectors of the two laser beams using the saturation technique [30–32], as described in our earlier papers

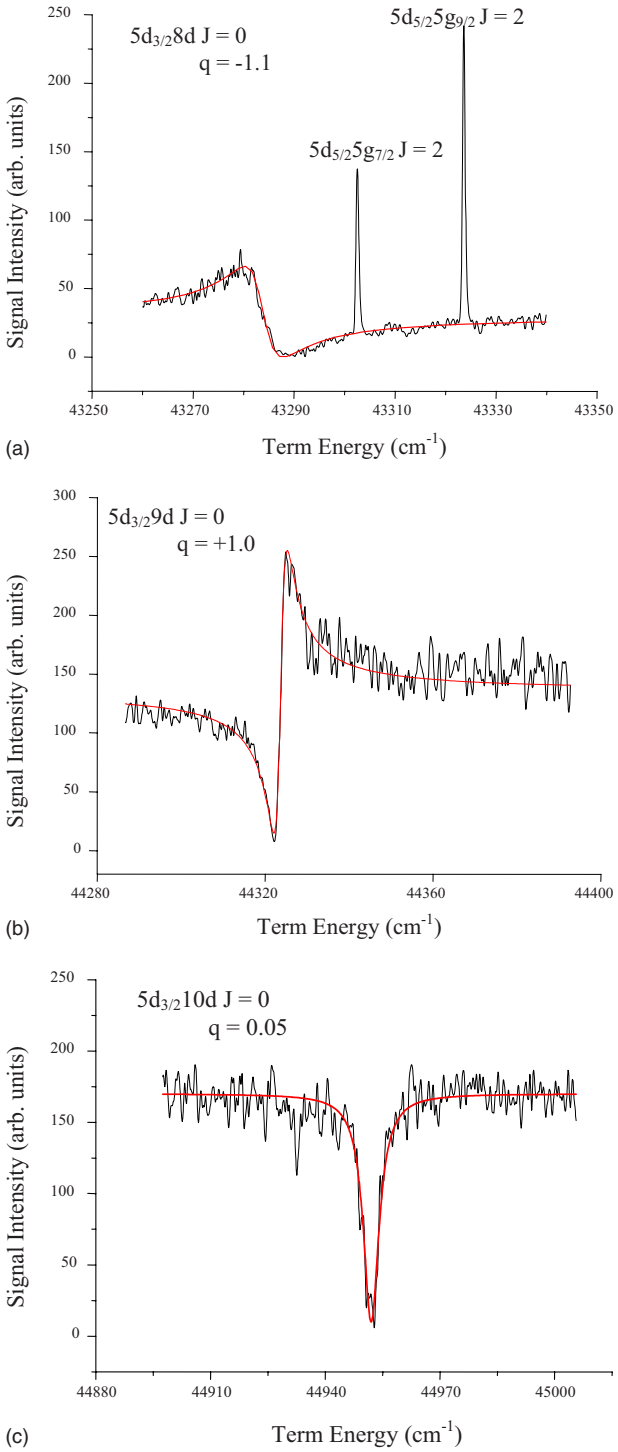

FIG. 4. (Color online) (a) A least-squares fit to the $5d_{3/2}8d$ $J=0$ autoionizing resonance of barium with negative line profile q parameter. The adjacent two sharp lines are the leading members of the ng series built on the $5d_{5/2}$ ionic level of barium. (b) A least-squares fit to the $5d_{3/2}9d$ $J=0$ autoionizing resonance of barium with positive line profile q parameter. (c) A least-squares fit to the $5d_{3/2}10d$ $J=0$ autoionizing resonance of barium with nearly zero line profile q parameter.

TABLE I. Fano parameters of the $J=0$ resonances in the vicinity of the $6p^2\ ^1S_0$ resonance.

	Present work			Keller *et al.* [29]	
Assignment	E (cm^{-1})	Γ (cm^{-1})	q	Γ (cm^{-1})	q
$6p^2\ ^1S_0$	44850.0	980	−5.4		
$5d_{3/2}8d$	43283.7	7.5	−1.1		
$5d_{3/2}9d$	44323.7	3.2	+1	3.3	+1.27
$5d_{3/2}10d$	44952.0	5.3	0		
$5d_{5/2}8d$	44118.0	5	−0.47	6.1	−0.80
$5d_{5/2}9d$	45116.0	54	0		

[33–36]. Keeping the intensity of the exciting laser sufficient to saturate the resonance transition for a pure two-step photoionization process, the number of ions per unit volume can be determined from the relation [30–33]

$$N = N_{ex}\left[1 - \exp\left(-\frac{\sigma U}{2\hbar\omega A}\right)\right]. \quad (2)$$

Here N_{ex} (cm^{-3}) is the density of the excited atoms, A (cm^2) is the cross-sectional area of the ionizing laser beam, U (joule) is the total energy per ionizing laser pulse, $\hbar\omega$ (joule) is the energy per photon of the ionizing laser beam, and σ (cm^2) is the absolute cross section for photoionization. All quantities in this relation are either known or can be measured except the number density N_{ex} and the photoionization cross section σ. These quantities can be determined by the least-squares fitting of Eq. (2) to the experimentally observed ionization signal data as a function of the ionizing laser energy density. The temporal overlapping of both the laser pulses is confirmed using a fast *p-i-n* photodiode (BPX65) at the entrance windows of the TOF. The area of the overlap region is calculated in the confocal limit within 10% error and the energy of the ionizing laser is measured by an energy meter (R-752, Universal Radiometer) within 3% error. Figure 5 shows the ionization signal versus the ionizing laser energy for the parallel and perpendicular polarizations of the two lasers. The solid line is the least-squares fit curve of Eq. (2) to the experimental data points to extract the photoionization cross section. The best fit to the experimental data points yields the photoionization cross section as $\sigma = 335 \pm 65$ Mb for the parallel polarization vectors whereas $\sigma = 215 \pm 45$ Mb when the polarizations of the two laser beams are perpendicular to each other. We have normalized the cross section for the entire region relative to these values. For the relative measurements, the intensity of the ionizing laser was kept constant throughout the scan and it was also ensured that no line gets saturated due to the laser power. Though we have tried to maintain the energy of the ionizing laser constant, yet 10% fluctuation is expected at both ends of a particular dye region. To avoid this fluctuation, we have recorded the spectra covering a small scanning region and a mixture of dyes was used to overlap the scanning region. Also the sample number density is necessary to remain uniform during the course of experiment which depends upon the working temperature of the furnace. The atomic beam oven temperature was kept stable at 900 K to ensure a constant number density. The temperature was monitored by a Ni-Cr-Ni thermocouple and was maintained within ±1% by a temperature controller. While recording the entire spectrum covered in the present experiment required for several hours, therefore, a gradual change in the vapor pressure of barium sample is unavoidable which may cause a systematic error in the relative measure-

TABLE II. Term energies of the $5d_{3/2,5/2}\ 7d$ and $8d$ configurations based lines. The effective quantum numbers have been calculated using the relation standard Rydberg relation using $d_{3/2}$ limit at 46 908.75 cm^{-1}, $d_{5/2}$ limit at 47 709.73 cm^{-1}, and Rydberg constant for barium=109 736.88 cm^{-1}.

Assignment	Term energy (cm^{-1})	Effective quantum number
$5d_{5/2}7d\ (5/2,3/2)_2$	41841.6	4.324
$5d_{5/2}7d\ (5/2,5/2)_2$	42118.0	4.430
$5d_{5/2}7d\ (5/2,5/2)_0$	42369.2	4.532
$5d_{3/2}8d\ (3/2,5/2)_1$	42878.6	5.218
$5d_{3/2}8d\ (3/2,5/2)_2$	43030.6	5.319
$5d_{3/2}8d\ (3/2,3/2)_1$	43089.7	5.360
$5d_{3/2}8d\ (3/2,3/2)_2$	43151.0	5.401
$5d_{3/2}8d\ (3/2,3/2)_0$	43283.7	5.502
$5d_{5/2}8d\ (5/2,3/2)_1$	43717.8	5.244
$5d_{5/2}8d\ (5/2,3/2)_2$	43800.9	5.298
$5d_{5/2}8d\ (5/2,5/2)_2$	44014.9	5.449
$5d_{5/2}8d\ (5/2,5/2)_0$	44118.0	5.529

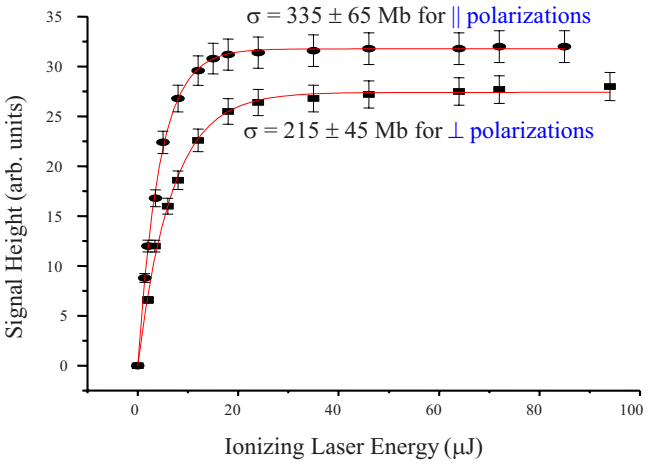

FIG. 5. (Color online) The photoionization data for the $5d6p\ ^1P_1$ excited state at the peak of the $5d7d\ (5/2,5/2)_2$ resonance. The solid line is the least-squares fit of Eq. (2) to the observed data for extracting the photoionization cross section. The 5% error bars on the data result from pulse-to-pulse fluctuations in the signal. The solid circles are the data points when the polarization vectors of the two lasers are parallel while the rectangular points are taken under the perpendicular polarizations of the two laser beams.

ments of the cross section, we introduce ≈10% error due to the variation in the laser power and an additional 5% error due to the variation in the vapor pressure. The overall uncertainty in the determination of the photoionization cross section does not exceed 20%. The absolute value of the photoionization cross section at the peak of the $6p^2\ ^1S_0$ autoionizing resonance is determined as 185 ± 35 Mb. Wood *et al.* [22] reported the photoionization cross section of barium for the $6s6p\ ^1P_1$ state at the peak of the $6p^2\ ^1S_0$ resonance as 450 Mb, in agreement to that experimentally measured value by Lange *et al.* [21]. However, Greene and Aymar [11] calculated the photoionization cross section for the $5d6p\ ^1P_1$ at the peak of the $6p^2\ ^1S_0$ resonance as 500 Mb using multichannel quantum defect theory and eigenchannel *R*-matrix approach. The present experimental value is nearly three times lower than that of the calculated value.

B. Multichannel quantum defect theory analysis

The optogalvonic spectrum of the $6p^2\ ^1S_0$ resonance reported by Aymar *et al.* [8] exhibits no Rydberg structure in the vicinity of this resonance except a single window type $5d_{3/2}10d_{3/2}$ resonance on the higher energy side of the broad $6p^2\ ^1S_0$ line. However, the calculated spectrum reveals some resonances corresponding to the 5*dnd* series on both sides of the broad resonance. Although there is an excellent agreement in the energy positions in the present work and the calculations of Aymar *et al.* [8], the line shapes of the resonances are rather different. In order to study the interaction of a continuum of finite bandwidth, the broad $6p^2\ ^1S_0$ profile in this treatment, with the 5*dnd* $J=0$ Rydberg series possessing same J values, we have performed calculations using MQDT formulated by Cooke and Cromer [37], Ueda [38] Gallagher [39], and Baig and Bhatti [40]. Since the channels possessing the same J values and same parity can interact, the $6p^2\ ^1S_0$ state can interact with the $(3/2,3/2)_0$ and $(5/2,5/2)_0$ series. We have performed a four-channel MQDT analysis considering the contribution of only $J=0$ channels. The MQDT technique requires the eigenquantum defect δ_i and the corresponding channel interaction parameters R_{ij}. Figure 6 shows a schematic indicating the three bound channels and one open channel used for the MQDT calculation. The $6s\ \varepsilon\ell$ channel is considered as an open channel attached to the 6*s* ionization threshold while the 5*dnd* $(3/2,3/2)_0$ channel 2, 5*dnd* $(5/2,5/2)_0$ channel 3, and 6*pnp* $^2P_{1/2,\ 3/2}$ channel 4 are considered as closed channels. The series limit associated with the 6*s* ionization threshold is taken as $I_{6s}=42\ 034.90\ \text{cm}^{-1}$ and that of associated with the $5d\ ^2D_{3/2}$, $5d\ ^2D_{5/2}$, and $6p\ ^2P_{1/2,\ 3/2}$ thresholds are taken as $46\ 908.75\ \text{cm}^{-1}$, $47\ 709.72\ \text{cm}^{-1}$, and $63\ 987.27\ \text{cm}^{-1}$, respectively. The four-channel MQDT equation can be written as [39]

$$\begin{vmatrix} \varepsilon_1 & R_{12} & R_{13} & R_{14} \\ R_{12} & \varepsilon_2 & R_{23} & R_{24} \\ R_{13} & R_{23} & \varepsilon_3 & R_{34} \\ R_{14} & R_{24} & R_{34} & \varepsilon_4 \end{vmatrix} = 0. \tag{3}$$

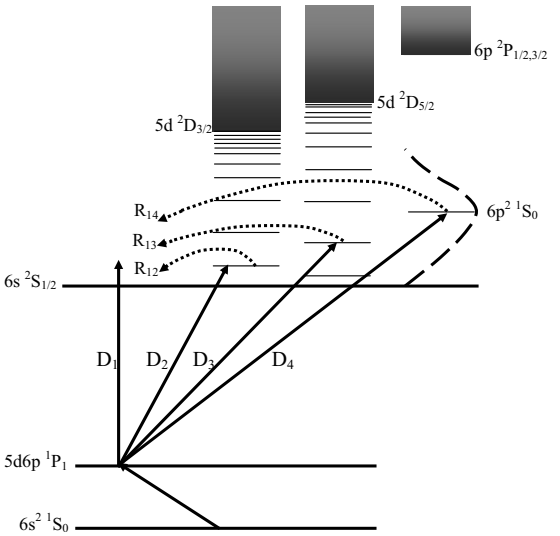

FIG. 6. Schematic indicating the three closed channels and one open channel used in the MQDT calculations.

Here R_{ij} describes the interaction between different channels and the diagonal terms ε_i are represented as $\varepsilon_i=\tan[\pi(\nu_i+\delta_i)]$, where ν_i is the effective quantum number with respect to the corresponding ionization limits and δ_i is the quantum defect. An expression to calculate the photoionization cross section for one open and three closed channels can be represented in terms of cofactors as (Baig and Bhatti [40]; Baig [41,42])

$$\sigma = 4\pi^2\alpha\hbar\omega \frac{\left|\sum_1^4 C_{1i}D_i\right|^2}{C_{11}^2 + \left|\sum_2^4 C_{1i}R_{1i}\right|^2}. \tag{4}$$

Here $\hbar\omega$ is the photon energy and D_i are the transition dipole moments between the initial state and the *i*th channel; R_{1i} are the interchannel interaction parameters that correspond to autoionization of the discrete levels of channels 2, 3, and 4 into the continuum; and C_{1i} are the cofactors of the first row of the MQDT matrix equation (3).

Figure 7 shows the experimentally recorded spectrum along with the simulated spectrum which reproduces the experimental data quite well. The energy positions and profiles of all the $J=0$ resonances in this region are in excellent agreement with the experimental spectrum; with an exception that the experimental width of the $5d9d\ [5/2,5/2]_0$ resonance is nearly five times larger than the calculated spectra. The different parameters extracted from the simulation of the spectrum are

$$\begin{array}{llll} R_{12}=0.15(2) & R_{23}=0.001(1) & D_1=2.0(2) & \delta_2=0.49(1) \\ R_{13}=0.15(2) & R_{24}=-0.01(1) & D_2=2.5(2) & \delta_3=0.47(1) \\ R_{14}=0.35(2) & R_{34}=-0.01(1) & D_3=3.0(3) & \delta_4=0.58(1) \\ & & D_4=9.1(5) & \end{array}.$$

The extra lines that appear in the experimental spectrum either belong to the 5*dnd* or 5*dng* series having $J=2$. As we

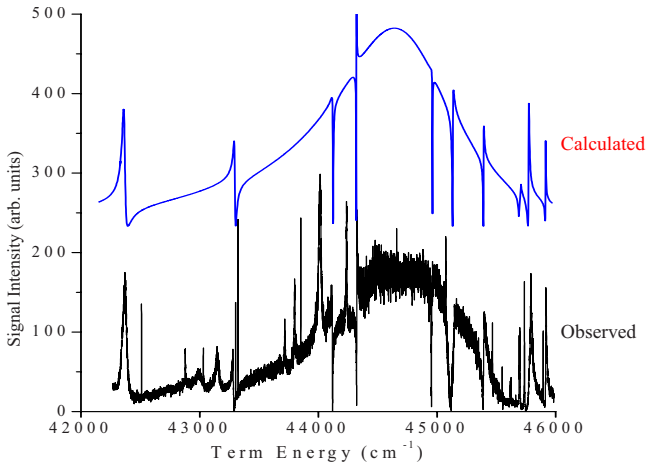

FIG. 7. (Color online) Experimentally recorded spectrum in the region 42 000–46 000 cm^{-1} showing the broad $6p^2\ ^1S_0$ autoionizing resonance. The base line of the four-channel MQDT simulated spectrum is shifted by 240 points to show the calculated line shapes of the autoionizing resonances.

have considered only the $J=0$ channels, therefore, these lines are missing in the simulated spectra. The large value of $R_{14}=0.35$ indicates that the dominant interaction in this region is between the $6p$ channel and the $6s\varepsilon\ell$ continuum while the value of the $R_{23}=0.001$ is negligibly small, which indicates that channels 2 and 3 are not coupled together. The next noticeable interaction is the interaction of channel 1 with channel 2 and channel 3, which is about half of the interaction between channel 4 and channel 1. The strength of interaction of channel 4 with channel 2 and channel 3 is nearly the same. Since D_i is the transition dipole moment between the initial state and the ith channel and the large value of $D_4=9.1$ (more than three times larger than that of the other channels) reflects that maximum photoionization occurs through the $6p^2$ channel. A comparison of the present calculated spectrum with that of the Aymar *et al.* [8] reveals that both the spectra are in excellent agreement as far as the energy positions of the resonances are concerned but the q parameters of the resonances are different. Our calculation covers the energy region 42 000–46 000 cm^{-1} whereas Aymar *et al.* [8] calculated a limited region that is why the complete line profile of the $6p^2\ ^1S_0$ could not be predicted in their calculations. Greene and Aymar [11] reported the partial photoionization cross section for the $5d6p\ ^1P_1 \rightarrow J=0^e$ symmetry of barium in the energy range 42 000–47 000 cm^{-1} using the multichannel quantum defect theory and eigenchannel R-matrix calculations in the LS and jj-coupling schemes (see Fig. 12 of their paper). The peak position of the $6p^2\ ^1S_0$ resonance coincides with our experimental spectra but their calculated width is much too small. In addition, the presently observed experimental line shapes of the $J=0$ Rydberg series attached to the $d_{3/2,5/2}$ limits considerably differ from their calculated spectrum. There is indeed a need to have more sophisticated calculations to compare the present experimental data.

IV. CONCLUSION

We report the true line shape of the $6p^2\ ^1S_0$ autoionizing resonance along with a complete spectrum from the $6s$ ionization threshold up to the $5d\ ^2D_{5/2}$ ionization threshold excited from the $5d6p\ ^1P_1$ intermediate level. The identification of the total angular momentum has been confirmed using the polarization selection rules of the laser radiation. A four-channel MQDT analysis has also been performed considering only the $J=0$ channels and an excellent agreement between the experimental data and the MQDT simulation is found for the position and line shape of the $6p^2\ ^1S_0$ resonance as well as for all the resonances in the vicinity of this broad resonance. Besides, we have extracted the line profile parameters for the $J=0$ autoionizing Rydberg series that sweep across the broad $6p^2\ ^1S_0$ resonance revealing an experimental example of the q-reversal phenomena. These experimental data on the line shape of the $6p^2\ ^1S_0$ resonance and the adjacent autoionizing resonances might stimulate some more theoretical calculations for the photoionization from the $5d6p\ ^1P_1$ state of barium.

ACKNOWLEDGMENTS

We are grateful to Quaid-i-Azam University Islamabad, Higher Education Commission (HEC) Pakistan, and Pakistan Science Foundation (Grant No. PSF-134) for financially supporting the research project.

[1] C. E. Moore, *Atomic Energy Levels*, Natl. Bur. Stand. (U.S.) Circ. (U.S. GPO, Washington, D.C., 1958), Vol. III.
[2] C. E. Moore, *Atomic Energy Levels*, Natl. Bur. Stand. (U.S.) Circ. (U.S. GPO, Washington, D.C., 1971), Vol. III.
[3] J. R. Rubbmark, S. A. Borgström, and K. Bockasten, J. Phys. B **10**, 421 (1977).
[4] M. Aymar, P. Camus, M. Dieulin, and C. Morillon, Phys. Rev. A **18**, 2173 (1978).
[5] J. J. Wynne and J. A. Armstrong, IBMJ Res. Div. **23**, 490 (1979).
[6] P. Camus, M. Dieulin, and El. A. Himdy, Phys. Rev. A **26**, 379 (1982).
[7] J. A. Armstrong, J. J. Wynne, and P. Esherick, J. Opt. Soc. Am. **69**, 211 (1979).
[8] M. Aymar, P. Camus, and A. El. Himdy, J. Phys. B **15**, L759 (1982).
[9] K. Bartschat, B. M. McLaughlin, and R. A. Hoversten, J. Phys. B **24**, 3359 (1991).
[10] K. Bartschat and C. H. Greene, J. Phys. B **26**, L109 (1993).
[11] C. H. Greene and M. Aymar, Phys. Rev. A **44**, 1773 (1991).
[12] C.-H. Li and D. Buker, Phys. Rev. A **74**, 012512 (2006).
[13] M. Saleem, N. Amin, S. Hussain, M. Rafiq, and M. A. Baig, Eur. Phys. J. D **38**, 277 (2006).
[14] M. Saleem, S. Hussain, M. Rafiq, and M. A. Baig, J. Appl. Phys. **100**, 053111 (2006).
[15] M. Rafiq, M. Saleem, S. Hussain, M. A. Kalyar, and M. A.

Baig, J. Phys. B **40**, 2291 (2007).
[16] D. Hanna, P. Karkainen, and R. Wyatt, Opt. Quantum Electron. **7**, 115 (1975).
[17] A. Yu. Elizarov and N. A. Cherepkov, Sov. Phys. JETP **69**, 695 (1989).
[18] P. H. Hechmann and E. Trabert, *Introduction to Spectroscopy of Atoms* (North-Holland, Amsterdam, 1989).
[19] L. O. Dickie and F. M. Kelly, Can. J. Phys. **49**, 2630 (1971).
[20] P. Camus, M. Dieulin, El. A. Himdy, and M. Aymar, Phys. Scr. **27**, 125 (1983).
[21] V. Lange, U. Eichmann, and W. Sandner, Phys. Rev. A **44**, 4737 (1991).
[22] R. P. Wood, C. H. Greene, and D. Armstrong, Phys. Rev. A **47**, 229 (1993).
[23] J. Neukammer, H. Rinneberg, G. Jonsson, W. E. Cooke, H. Hieronymus, A. Konig, K. Vietzke, and H. Spinger-Bolk, Phys. Rev. Lett. **55**, 1979 (1985).
[24] H. Hieronymus, J. Neukammer, and H. Rinneberg, J. Phys. B **25**, 3463 (1992).
[25] U. Fano, Phys. Rev. **124**, 1866 (1961).
[26] J. P. Connerade, Proc. R. Soc. London, Ser. A **362**, 361 (1978).
[27] M. A. Baig and J. P. Connerade, J. Phys. B **18**, 3487 (1985).
[28] J. P. Connerade, A. M. Lane, and M. A. Baig, J. Phys. B **18**, 3507 (1985).
[29] J. S. Keller, J. E. Hunter III, and R. S. Berry, Phys. Rev. A **43**, 2270 (1991).
[30] C. E. Burkhardt, J. L. Libbert, J. Xu, J. J. Leventhal, and J. D. Kelley, Phys. Rev. A **38**, 5949 (1988).
[31] B. Willke and M. Kock, Phys. Rev. A **43**, 6433 (1991).
[32] L.-W. He, C. E. Burkhardt, C. Ciocca, J. J. Laventhal, H.-L. Zhou, and S. T. Manson, Phys. Rev. A **51**, 2085 (1995).
[33] M. Saleem, S. Hussain, M. Rafiq, and M. A. Baig, J. Phys. B **39**, 5025 (2006).
[34] M. A. Kalyar, M. Rafiq, Sami-ul Haq, and M. A. Baig, J. Phys. B **40**, 2307 (2007).
[35] M. A. Baig, S. Mahmood, M. Rafia, M. Rafiq, M. A. Kalyar, S. Hussain, and R. Ali, Phys. Rev. A **78**, 032524 (2008).
[36] M. Saleem, S. Hussain, and M. A. Baig, Phys. Rev. A **77**, 062506 (2008).
[37] W. E. Cooke and C. L. Cromer, Phys. Rev. A **32**, 2725 (1985).
[38] K. Ueda, Phys. Rev. A **35**, 2484 (1987).
[39] T. F. Gallagher, *Rydberg Atoms* (Cambridge University Press, Cambridge, England, 1994).
[40] M. A. Baig and S. A. Bhatti, Phys. Rev. A **50**, 2750 (1994).
[41] M. A. Baig, Eur. Phys. J. D **46**, 437 (2008).
[42] M. A. Baig, Phys. Rev. A **79**, 012509 (2009).